Table 4. Total frequencies and probabilities of sense and complementary sequences of non-ribosomal, non-V00125 and random hexanucleotides in reported sequences of mammalian ribosomal RNAs and satellite repeat

Accession	Molecule	Species	Sequence length	Non-ribosomal Frequencies	Probabilities ($\times 10^{-3}$)	Non-V00125 Frequencies	Probabilities ($\times 10^{-3}$)	Random Frequencies	Probabilities ($\times 10^{-3}$)
X00686	18S rRNA	*Mus musculus*	1869	27	7.22	101	27.02	85.4	22.85
X82564	45S pre rRNA gene	*M.musculus*	22 118	281	6.35	897	20.28	974.8	22.04
M11188	18S rRNA gene. Complete	*Rattus norvegicus*	1920	27	7.03	107	27.86	87	22.66
M10098	18S rRNA gene. Complete	*Homo sapiens*	1969	27	6.86	108	27.43	89.6	22.75
U13369	Complete repeating unit	*H.sapiens*	42 999	203	2.36	1569	18.24	1743.4	20.27
M27830	28S rRNA gene. Complete	*H.sapiens*	1955	9	2.30	53	13.55	82.4	21.07
X14345	5′ external transcribed spacer of pre-ribosomal RNA	*H.sapiens*	3627	2	0.28	108	14.89	176.6	24.35
AY265350	18S rRNA gene. Complete	*S.scrofa*	2302	25	5.43	114	24.76	105.4	22.89
V01270	18S 5.8S and 28S rRNA	*R.norvegicus*	8647	71	4.11	351	20.30	405	23.42
X01117	18S rRNA sequence	*R.norvegicus*	1874	27	7.20	100	26.68	84.8	22.63
AJ311674	Partial 18S rRNA gene	*Dasypus novemcinctus*	1824	27	7.40	99	27.14	83.2	22.81
AJ311675	Partial 18S rRNA gene	*Erinaceus europaeus*	1825	27	7.40	101	27.67	82.4	22.58
AJ311673	Partial 18S rRNA gene	*Equus caballus*	1824	25	6.85	100	27.41	82.8	22.70
X06778	18S rRNA	*Oryctolagus cuniculus*	1863	30	8.05	103	27.64	84.6	22.71
AJ311678	Partial 18S rRNA gene	*Vombatus ursinus*	1845	28	7.59	101	27.37	81.8	22.17
AJ311676	Partial 18S rRNA gene	*Monodelphis domestica*	1847	28	7.58	100	27.07	81.6	22.09
AJ311677	Partial 18S rRNA gene	*Didelphis virginiana*	1847	28	7.58	100	27.07	81.6	22.09
AJ311679	Partial 18S rRNA gene	*Ornithorhynchus anatinus*	1850	28	7.57	102	27.57	82.8	22.38
V00125	Repeated unit of bovine 1.715 satellite DNA	*Bos taurus*	1399	0	0.00	0	0.00	66.6	23.80
J00036	Thymus satellite I	*B.taurus*	1402	3	1.07	5	1.78	64.2	22.90
U59381	Tetranucleotide microsatellite repeat	*H.sapiens*	1032	2	0.97	29	14.05	35	16.96
AY153482	Microsatellite PDE6B sequence	*S.scrofa*	1895	20	5.28	64	16.89	82.6	21.79
AF298194	Clone pW-1 microsatellite III	*H.sapiens*	1524	17	5.58	31	10.17	71	23.29
AY339973	Clone 1 satellite sequence	*Canis familiaris*	1200	17	7.08	41	17.08	52.6	21.92
U53349	Chromosome 10 microsatellite	*R.norvegicus*	1070	21	9.81	32	14.95	36.2	16.92
AJ295050	Alpha satellite 5CEN-P7	*H.sapiens*	1382	31	11.22	61	22.07	58.8	21.27
AB023433	Satellite sequence	*R.norvegicus*	2845	86	15.11	136	23.90	125	21.97
AY145450	Microsatellites D6Wum35 and D6Wum34	*M.musculus*	1704	71	20.83	103	30.22	73.4	21.54
AF181667	Polymorphic microsatellite sequence	*H.sapiens*	3650	201	27.53	213	29.18	164.4	22.52
AF259760	Microsatellite MNS-87 and MNS-88	*Ovis aries*	1074	86	40.04	38	17.69	48.2	22.44
U10629	Chromosome 4 satellite	*H.sapiens*	1060	116	54.72	48	22.64	55.4	26.13

Sequences of the non-V00125 and random hexamers are supplemented online. Probabilities of the hexanucleotide-sets in 2464 reported satellite repeat are also supplemented online.

Table 5. Number of species and maximum, minimum and median probabilities [median (minimum maximum)] ($\times 10^{-3}$) of non-ribosomal, non-V00125-satellite-repeat and random hexamers hexanucleotides in known viral species

Family	Number of species	Non-ribosomal	Non-V00125	Random hexamers
Adenoviridae	25	15.3 (6.5–28.3)	25.0 (19.4–47.1)	23.8 (22.8–47.6)
Arenaviridae	8	17.0 (13.1–19.2)	26.0 (23.3–27.6)	24.5 (23.8–25.1)
Astroviridae	7	17.4 (14.5–19.2)	23.9 (22.4–25.6)	24.3 (23.5–25.2)
Bornaviridae	1	20.0 (20.0–20.0)	21.8 (21.8–21.8)	23.7 (23.7–23.7)
Bunyaviridae	26	22.8 (11.8–30.7)	26.2 (21.8–29.7)	23.7 (23.1–25.3)
Caliciviridae	23	13.2 (7.1–19.3)	23.5 (19.1–26.5)	24.1 (23.4–25.4)
Coronaviridae	51	24.2 (23.9–31.4)	25.3 (25.2–29.9)	23.6 (23.5–24.3)
Filoviridae	3	21.9 (20.8–22.6)	24.9 (24.4–26.2)	25.0 (24.5–25.1)
Flaviviridae	53	14.1 (8.6–23.4)	22.4 (19.0–25.9)	24.0 (21.6–25.2)
Hepadnaviridae	14	16.6 (9.7–27.2)	21.6 (18.0–25.3)	24.0 (21.3–24.5)
Herpesviridae	31	15.0 (3.7–29.2)	22.6 (16.4–27.2)	23.5 (22.8–24.5)
Iridoviridae	3	17.7 (14.1–25.2)	23.3 (20.8–29.3)	23.5 (21.9–23.6)
Orthomyxoviridae	1029	17.6 (6.3–29.7)	24.3 (16.2–32.9)	24.3 (20.0–27.9)
Papillomaviridae	123	24.7 (7.7–34.3)	24.9 (18.7–28.9)	23.2 (21.1–25.0)
Parvoviridae	59	20.5 (6.3–35.9)	25.0 (19.5–31.2)	23.8 (21.6–25.1)
Picornaviridae	90	19.3 (7.1–30.6)	24.3 (19.0–29.0)	24.0 (22.6–25.1)
Polyomaviridae	16	18.4 (14.0–28.5)	22.0 (20.6–26.4)	23.6 (22.3–24.7)
Poxviridae	21	37.6 (8.2–44.8)	26.9 (22.7–32.0)	22.9 (21.3–24.0)
Reoviridae	89	28.4 (12.9–38.4)	26.2 (19.2–31.5)	23.8 (20.7–25.8)
Retroviridae	86	17.0 (9.9–27.6)	22.1 (18.2–26.8)	23.3 (21.6–24.6)
Rhabdoviridae	14	16.8 (9.2–25.3)	22.7 (19.0–26.3)	23.6 (23.1–24.2)
Togaviridae	19	20.0 (7.6–24.3)	23.3 (20.1–25.1)	23.7 (22.7–24.5)

Sequences for species were selected according to their length as described in Materials and Methods. The total probability in each species was calculated as the summation of probabilities of all non-ribosomal hexanucleotides in sense and complementary sequences of a viral genomic sequence that was selected as described in Materials and Methods. The probabilities of non-ribosomal hexanucleotides in 1791 virus genomic sequences are supplemented online.

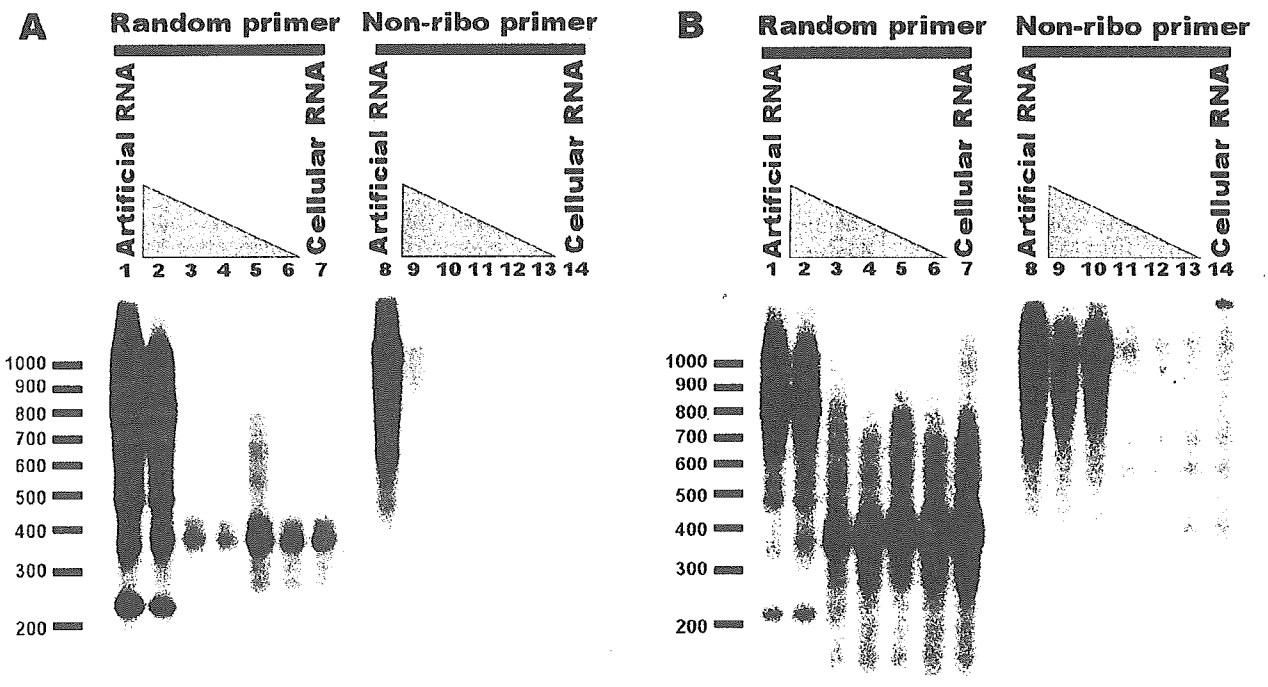

Figure 2. Autoradiogram of ^{32}P-labelled double-stranded cDNA synthesized from mixtures consisting of artificial RNA and total cellular RNA. *In vitro* transcribed RNA was synthesized from pCIneo plasmid and mixed with total cellular RNA extracted from rat2 cells in weight proportions 1:0 (lanes 1 and 8), 1:1 (lanes 2 and 9), 1:10 (lanes 3 and 10), 1:100 (lanes 4 and 11), 1:300 (lanes 5 and 12), 1:1000 (lanes 6 and 13) and 0:1 (lanes 7 and 14). One microgram of mixed RNA was reverse transcribed using random (lanes 1–7) or non-ribosomal (lanes 8–14) hexanucleotides and a second-strand cDNA was then synthesized with RNaseH, DNA polymerase and DNA ligase according to the method described in Materials and Methods. One-tenth of the volume of synthesized cDNAs was loaded on agarose gel (**A**). Loaded volumes were corrected to include the same amounts of ^{32}P in each sample (**B**). Positions and sizes (bp) of markers are present on the left.

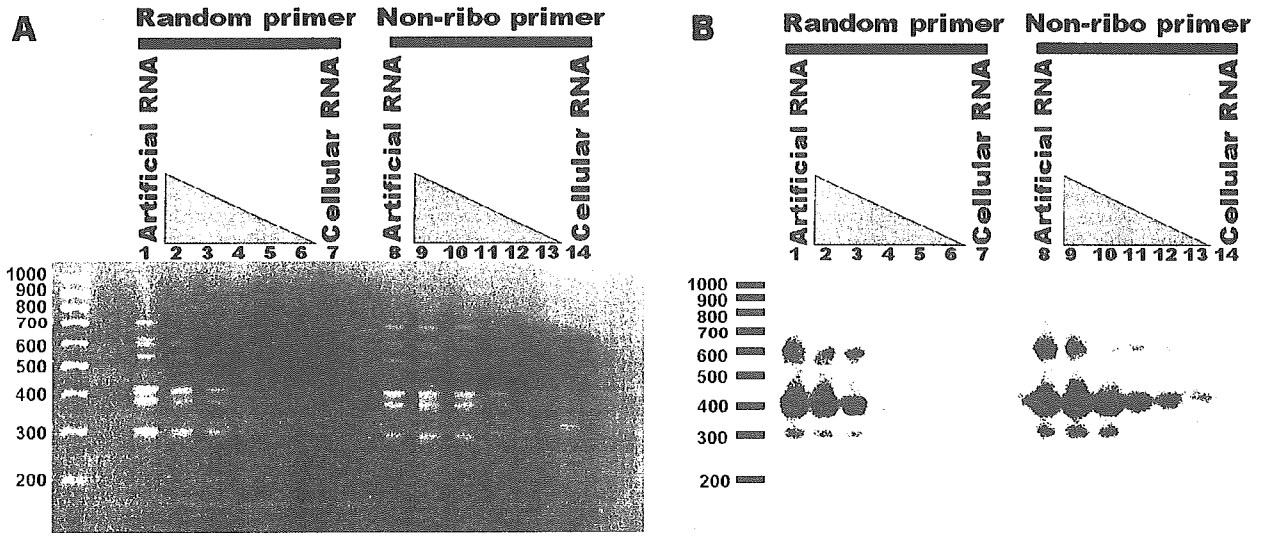

Figure 3. Agarose gel electrophoresis of RDA products (**A**) and its hybridized autoradiogram (**B**). *In vitro* transcribed RNA and total cellular RNA were mixed as described in the legend to Figure 2. Double-stranded cDNAs were synthesized and subjected to RDA as described in Materials and Methods. One-twentieth of the volume of the amplified products was separated on 3% agarose gel and stained with ethidium bromide (**A**), blotted onto a nylon membrane and hybridized with ^{32}P-labelled pCIneo (**B**). Positions and sizes (bp) of markers are present on the left.

On the other hand, the synthesis of ribosomal cDNA was not obvious in the cDNA primed with non-ribosomal hexanucleotides. A relatively large cDNA derived from artificial RNA could be observed even when a smaller proportion of test RNA was mixed with cellular RNA and non-ribosomal hexanucleotide-primed samples. These data suggest that the relative amount of test RNA-derived cDNA is greater in non-ribosomal hexanucleotides-primed samples than in random primer-primed samples.

After the first round of cDNA RDA, amplified fragments were observed on agarose by staining with ethidium bromide. The bands that corresponded to artificial RNA could be observed in 1:0, 1:1 and 1:10 (test:total cellular RNAs) mixtures when cDNAs were primed with a random primer. On the other hand, these bands could be observed in 1:0 to 1:300 RNA mixtures when cDNA was primed with non-ribosomal hexanucleotides (Figure 3A). This amplification of test RNA was confirmed by hybridization with pCIneo, which was a template for *in vitro* RNA synthesis (Figure 3B). The hybridized bands were observed even in a lane corresponding to 1:1000 RNA mixture. When cDNA was primed with a random primer, the hybridized bands could not be observed in 1:100, 1:300 and 1:1000 RNA mixtures. These data suggest that the lower limit of the test RNA amplification decreased at least 30 times when non-ribosomal hexanucleotides were used for reverse transcription when compared with the data obtained by using a random primer.

Detection of BPI3 and SARS-CoV sequences from infected cell RNA

To amplify virus sequence from infected cells, we subtracted amplicons derived from uninfected cells from those derived from virus-infected cells. Amplicons with linkers derived from the infected cells were mixed with amplicons without linkers

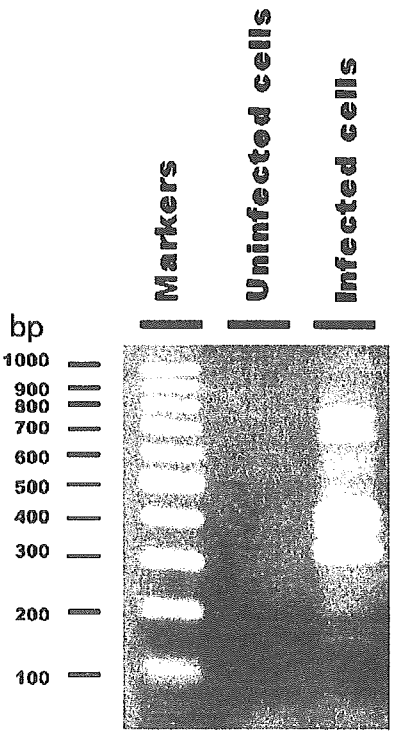

Figure 4. Agarose gel electrophoresis of RDA products from RNA extracted from bovine parainfluenza virus 3-infected cells. Double-stranded cDNA was synthesized from RNA of bovine parainfluenza virus 3-infected MDBK cells and subjected to RDA. Mock-infected cells were used for the synthesis of driver amplicons for RDA. One-twentieth of the volume of the amplified products was separated on 3% agarose gel and stained with ethidium bromide. RDA product from the uninfected control cells was used as a negative control.

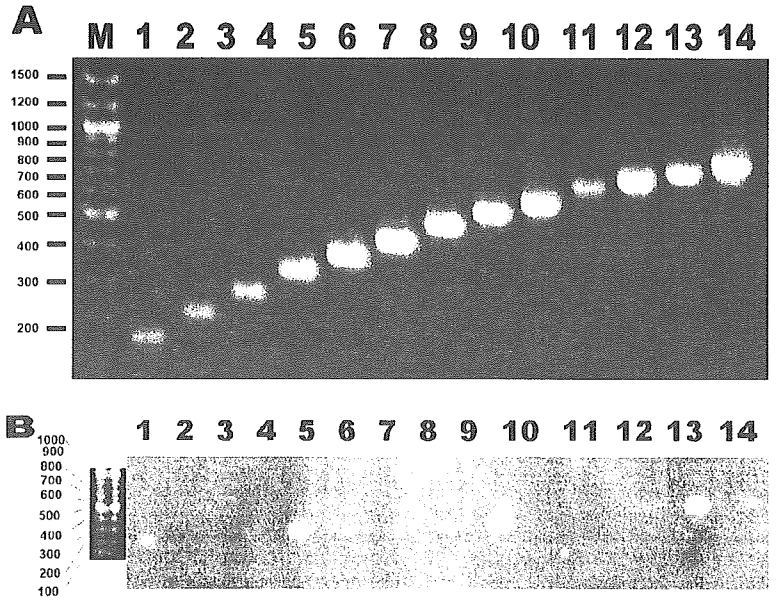

Figure 5. Agarose gel electrophoresis of RDA products with PCR products used for probes for hybridization (**A**) and a hybridized fluorogram (**B**). RNA was extracted from SARS-CoV-infected cells and subjected to RDA according to the method described in Materials and Methods. Mock-infected cells were used for the synthesis of driver amplicons for RDA. One-twentieth of the volume of the amplified products was separated on 3% agarose gels and blotted on a Nylon membrane. The membrane was then cut into slits that contained the lane showing the presence of DNA. On the other hand, the PCR fragments predicted to be amplified in the RDA reaction were amplified and subsequently ascertained by agarose gel electrophoresis (A). The amplified genomic fragments of SARS-CoV were Dig-labelled and used as probes for hybridization to each slit of the Nylon membrane containing the RDA product. Hybridization was performed in separate hybridization bags. After washing with 1× SSC and 0.1% SDS solution, the hybridized probes were detected on a fluorogram (B). Positions and sizes (bp) of markers are present on the left.

derived from uninfected cells at the ratio of 1:100 before a hybridization step of cDNA RDA. At the end of the first round of cDNA RDA, the ladders of amplified fragments were generated from BPI3-infected cells when non-ribosomal hexanucleotides were used (Figure 4). No cDNA RDA-derived bands were obvious when a random primer was used for reverse transcription (data not shown). Amplified fragments from cDNA RDA of BPI3-infected cells were cloned into pSPORT1 plasmid, and the sequences were determined. The sequences of all the cloned fragments from cDNA RDA were identical to the sequence of the BPI3 genome. These data suggest that cDNA RDA with non-ribosomal hexanucleotides enables the identification of the BPI3 genome sequence from infected cells.

Similar to BPI3, cDNA fragments derived from SARS-CoV were also amplified from SARS-CoV-infected cells (Figure 5). Viral origin of the amplified fragments was confirmed by hybridization (Figure 5B) and PCR amplification by SARS-CoV-specific primers (Figure 5A). These results indicate that genomic fragments of SARS-CoV can also be isolated by this method.

DISCUSSION

Reduction of influence of ribosomal RNA on cDNA synthesis by non-ribosomal hexanucleotides

It is well known that 3–5% and 30% of cellular RNA are estimated to be messenger and ribosomal RNA, respectively. The frequency of ribosomal RNA has been estimated by competitive PCR and real-time PCR to be 10 000 copies per cell (18). The amount of ribosomal RNA has been reported to be 1000-fold greater than that of frequently transcribed mRNA, such as beta actin and G6PDH. Thus, the repertoire of cDNA would be strongly affected by ribosomal RNA. This influence of ribosomal RNA has been avoided by oligo(dT) selection. Alternative strategy for the elimination of ribosomal RNA from total RNA, however, has not been developed. Therefore, there have been only a few applications of cDNA RDA for non-poly(A) RNA, such as those in viral genomes. In this study, we developed a new strategy for the elimination of ribosomal RNA in cDNA RDA through the construction of a hexanucleotide mixture and demonstrated its efficiency in cDNA RDA.

The main purpose of PCR is specific amplification of a gene. However, methods using multiple primers for simultaneous gene amplification have been recently employed for DNA chip methods. In order to simultaneously detect multiple genes by using a DNA chip, mixed oligonucleotides have been used as a primer for reverse transcription. This usage of mixed primers was based on the assumption that the specificity of primers was equal to the summation of the specificity of each primer. Thus, we searched for primers that do not prime ribosomal RNAs by frequency analysis of hexanucleotides. The frequency and distribution of oligonucleotides in mammalian and viral genomes have been studied to search for common motifs that might be used for controlling cellular functions (19–23). Volinia *et al.* (22) found sets of common decamers that can be used for the control of transcription control signals or for the common amplification of viruses. Programs for frequency

analysis have been useful for searching common oligonucleotides in many subsets of sequences. On the other hand, database programming is useful not only for searching common oligonucleotides but also for searching oligonucleotides that do not exist in a subset of sequences. In this study, we found that there were hexanucleotide patterns that were rare or that did not exist in ribosomal RNA sequences. We also showed that sequences of 96 selected non-ribosomal hexanucleotides are normally present in known viral sequences (Table 5).

Improvement of detection efficiency of extracellular RNA on cDNA RDA

In the experiment for the determination of the effect of non-ribosomal hexanucleotides, we used a mixture of artificially synthesized and total cellular RNAs. The probabilities of hexanucleotide patterns in the sequence of pCIneo was different from ribosomal RNA (18.4×10^{-3}, 22.4×10^{-3} and 23.0×10^{-3} for non-ribosomal, non-V00125 and random hexamers, respectively). The artificially synthesized RNA included 30 priming sites for non-ribosomal hexanucleotides and was efficiently reverse transcribed (Figure 2). In the model experiments, cDNA RDA with non-ribosomal hexanucleotides efficiently reverse transcribed and specifically amplified the extracellular test RNA in the mixed RNA (Figure 3). cDNA RDA-derived detection of the artificial RNA was 30-fold more sensitive when non-ribosomal hexanucleotides were used than when random hexamers were used. These results suggest that non-ribosomal hexanucleotides dramatically improve the detection efficiency of cDNA RDA.

Application of non-ribosomal hexanucleotides for viral detection

The common existence of non-ribosomal hexanucleotides in known viral genomes (Table 5) and the improved sensitivity for the amplification of a non-ribosomal sequence in the mixed RNAs (Figure 3) suggest that non-ribosomal hexanucleotides could be used for non-specific detection of a viral sequence in infected cells. However, the sensitivity for sequence detection may be low when compared with that of common PCR using specific primers. Thus, the usage of this method might be restricted to infected cells that contain many copies of a virus.

The copy number of RNA viruses is dependent on the virus species, host cells and replicative and productive state of viruses. In our experiment, we detected 3 ng of contaminated RNAs in 1 μg of total RNA. Although this sensitivity is considerably lower than that of normal PCR, our experiments on SARS-CoV and BPI3 suggest that the sensitivity of cDNA RDA with non-ribosomal hexanucleotides is sufficient to detect these viruses in productively infected cells. Additionally, this method can be applied to most productive viruses, since sense and complementary sequences of non-ribosomal hexanucleotides were found to exist in most of the known virus sequences in GenBank (Table 5). In conclusion, this method could be applied as an alternative method for the detection of any emerging viruses.

SUPPLEMENTARY MATERIAL

Supplementary Material is available at NAR Online.

ACKNOWLEDGEMENTS

This work was funded by a grant from the Ministry of Economy, Trade and Industry of Japan (to D.E.) and by a grant from the Ministry of Environment of Japan. Funding to pay the Open Access publication charges for this article was provided by New Industry Creative Type Technology R&D Promotion Program in the Hokkaido Bureau of Economy, Trade and Industry.

Conflict of interest statement. None declared.

REFERENCES

1. Rota,P.A., Oberste,M.S., Monroe,S.S., Nix,W.A., Campagnoli,R., Icenogle,J.P., Penaranda,S., Bankamp,B., Maher,K., Chen,M.H. *et al.* (2003) Characterization of a novel coronavirus associated with severe acute respiratory syndrome. *Science*, **300**, 1394–1399.
2. Gao,S.J. and Moore,P.S. (1996) Molecular approaches to the identification of unculturable infectious agents. *Emerg. Infect. Dis.*, **2**, 159–167.
3. Holmes,E.C. and Rambaut,A. (2004) Viral evolution and the emergence of SARS coronavirus. *Philos. Trans. R. Soc. Lond., B, Biol. Sci.*, **359**, 1059–1065.
4. Pavlovic-Lazetic,G.M., Mitic,N.S. and Beljanski,M.V. (2004) Bioinformatics analysis of SARS coronavirus genome polymorphism. *BMC Bioinformatics*, **5**, 65.
5. Lisitsyn,N., Lisitsyn,N. and Wigler,M. (1993) Cloning the differences between two complex genomes. *Science*, **259**, 946–951.
6. Chang,Y., Cesarman,E., Pessin,M.S., Lee,F., Culpepper,J., Knowles,D.M. and Moore,P.S. (1994) Identification of herpesvirus-like DNA sequences in AIDS-associated Kaposi's sarcoma. *Science*, **266**, 1865–1869.
7. Staskus,K.A., Zhong,W., Gebhard,K., Herndier,B., Wang,H., Renne,R., Beneke,J., Pudney,J., Anderson,D.J., Ganem,D. *et al.* (1997) Kaposi's sarcoma-associated herpesvirus gene expression in endothelial (spindle) tumor cells. *J. Virol.*, **71**, 715–719.
8. Hubank,M. and Schatz,D.G. (1994) Identifying differences in mRNA expression by representational difference analysis of cDNA. *Nucleic Acids Res.*, **22**, 5640–5648.
9. Tian,H., Cao,L., Tan,Y., Williams,S., Chen,L., Matray,T., Chenna,A., Moore,S., Hernandez,V., Xiao,V. *et al.* (2004) Multiplex mRNA assay using electrophoretic tags for high-throughput gene expression analysis. *Nucleic Acids Res.*, **32**, e126.
10. Eldering,E., Spek,C.A., Aberson,H.L., Grummels,A., Derks,I.A., de Vos,A.F., McElgunn,C.J. and Schouten,J.P. (2003) Expression profiling via novel multiplex assay allows rapid assessment of gene regulation in defined signalling pathways. *Nucleic Acids Res.*, **31**, e153.
11. Bailly,J.E., McAuliffe,J.M., Skiadopoulos,M.H., Collins,P.L. and Murphy,B.R. (2000) Sequence determination and molecular analysis of two strains of bovine parainfluenza virus type 3 that are attenuated for primates. *Virus Genes*, **20**, 173–182.
12. Iwai,H., Morioka,A., Shoya,Y., Obata,Y., Goto,M., Kirisawa,R., Okada,H. and Yoshino,T. (1998) Protective effect of passive immunization against TNF-alpha in mice infected with Sendai virus. *Exp. Anim.*, **47**, 49–54.
13. Mizutani,T., Fukushi,S., Saijo,M., Kurane,I. and Morikawa,S. (2004) Importance of Akt signaling pathway for apoptosis in SARS-CoV-infected Vero E6 cells. *Virology*, **327**, 169–174.
14. Mizutani,T., Fukushi,S., Saijo,M., Kurane,I. and Morikawa,S. (2004) Phosphorylation of p38 MAPK and its downstream targets in SARS coronavirus-infected cells. *Biochem. Biophys. Res. Commun.*, **319**, 1228–1234.
15. Mizutani,T., Fukushi,S., Murakami,M., Hirano,T., Saijo,M., Kurane,I. and Morikawa,S. (2004) Tyrosine dephosphorylation of STAT3 in SARS coronavirus-infected Vero E6 cells. *FEBS Lett.*, **577**, 187–192.
16. Thiel,V., Ivanov,K.A., Putics,A., Hertzig,T., Schelle,B., Bayer,S., Weissbrich,B., Snijder,E.J., Rabenau,H., Doerr,H.W. *et al.* (2003) Mechanisms and enzymes involved in SARS coronavirus genome expression. *J. Gen. Virol.*, **84**, 2305–2315.
17. Hubank,M. and Schatz,D.G. (1994) Identifying differences in mRNA expression by representational difference analysis of cDNA. *Nucleic Acids Res.*, **22**, 5640–5648.

18. Monk,R.J., Meyuhas,O. and Perry,R.P. (1981) Mammals have multiple genes for individual ribosomal proteins. *Cell*, **24**, 301–306.
19. Gambari,R., Volinia,S., Nesti,C., Scapoli,C. and Barrai,I. (1994) A set of Alu-free frequent decamers from mammalian genomes enriched in transcription factor signals. *Comput. Appl. Biosci.*, **10**, 501–508.
20. Scapoli,C., Rodriguez-Larralde,A., Volinia,S. and Barrai,I. (1993) Enrichment of oligonucleotide sets with transcription control signals. III: DNA from non-mammalian vertebrates. *Comput. Appl. Biosci.*, **9**, 647–651.
21. Scapoli,C., Rodriguez-Larralde,A., Volinia,S., Beretta,M. and Barrai,I. (1994) Identification of a set of frequent decanucleotides in plants and in animals. *Comput. Appl. Biosci.*, **10**, 465–470.
22. Volinia,S., Scapoli,C., Gambari,R., Barale,R. and Barrai,I. (1991) A set of viral DNA decamers enriched in transcription control signals. *Nucleic Acids Res.*, **19**, 3733–3740.
23. Volinia,S., Scapoli,C., Gambari,R., Barale,R. and Barrai,I. (1992) Enrichment of oligonucleotide sets with transcription control signals. II: Mammalian DNA. *Nucleic Acids Res.*, **20**, 551–556.

DTD 5

Available online at www.sciencedirect.com
SCIENCE DIRECT®

Journal of Virological Methods xxx (2005) xxx–xxx

Journal of Virological Methods

www.elsevier.com/locate/jviromet

Recombinant nucleocapsid protein-based IgG enzyme-linked immunosorbent assay for the serological diagnosis of SARS

Masayuki Saijo[a,*], Toshio Ogino[b], Fumihiro Taguchi[b], Shuetsu Fukushi[a], Tetsuya Mizutani[a], Tsugunori Notomi[c], Hidetoshi Kanda[c], Harumi Minekawa[c], Shutoku Matsuyama[b], Hoang Thuy Long[d], Nguyen Thi Hong Hanh[d], Ichiro Kurane[a], Masato Tashiro[b], Shigeru Morikawa[a]

[a] *Special Pathogens Laboratory, Department of Virology 1, National Institute of Infectious Diseases, 4-7-1 Gakuen, Musashimurayama 208-0011, Tokyo, Japan*
[b] *Laboratory of Respiratory Viral Diseases and SARS, Department of Virology 3, National Institute of Infectious Diseases, 4-7-1 Gakuen, Musashimurayama 208-0011, Tokyo, Japan*
[c] *Biochemical Research Laboratory, Eiken Chemical Co., Ltd., 1381-3 Shimoishigami, Ohtawara, Tochigi 324-0036, Japan*
[d] *National Institute of Hygiene and Epidemiology, 1, Yersin Street, Hanoi, Vietnam*

Received 6 October 2004; received in revised form 19 January 2005; accepted 26 January 2005

Abstract

The recombinant nucleocapsid protein (rNP) of severe acute respiratory syndrome (SARS) coronavirus (SARS-CoV) was expressed in a baculovirus system. The purified SARS-CoV rNP was used as an antigen for detection of SARS-CoV antibodies in IgG enzyme-linked immunosorbent assay (ELISA). The ELISA was evaluated in comparison with neutralizing antibody assay and the authentic SARS-CoV antigen-based IgG ELISA. Two-hundred and seventy-six serum samples were collected from health care workers in a hospital in which a nosocomial SARS outbreak took place and used for evaluation. The SARS-CoV rNP-based IgG ELISA has 92% of sensitivity and specificity compared with the neutralizing antibody assay and 94% sensitivity and specificity compared with the authentic SARS-CoV antigen-based IgG ELISA. The results suggest that the newly developed SARS-CoV rNP-based IgG ELISA is a valuable tool for the diagnosis and seroepidemiological study of SARS. The SARS-CoV rNP-based IgG ELISA has an advantage over the conventional IgG ELISA in that the antigen can be prepared by laboratory workers without the risk of infection.

Keywords: Recombinant nucleocapsid protein; SARS; IgG ELISA; Neutralizing antibody assay

1. Introduction

Severe acute respiratory syndrome (SARS), an emerging virus infection of the respiratory organs with a high mortality rate in humans, was first reported in Guangdong province, in southern part of China, in November 2002 and spread to Hong Kong, Vietnam, Singapore and other countries worldwide through human-to-human transmission (CDC, 2003; Lee et al., 2003; Poutanen et al., 2003; Tsang et al., 2003). Approximately 8000 patients were reported and about 800 died in the last SARS outbreak from November 2002 to July 2003 (WHO).

The causative agent, SARS coronavirus (SARS-CoV), was isolated from patients with SARS and was identified as a novel coronavirus. SARS-CoV was transmitted from human to human, and the mortality rate is high. SARS-CoV is regarded as a viral pathogen that must be handled in high containment laboratories with a biosafety level (BSL)-3 and BSL-4.

If a recombinant protein of SARS-CoV can be used as an antigen for serological diagnosis of SARS-CoV infections,

* Corresponding author. Tel.: +81 42 561 0771; fax: +81 42 561 2039.
E-mail address: msaijo@nih.go.jp (M. Saijo).

0166-0934/$ – see front matter © 2005 Elsevier B.V. All rights reserved.
doi:10.1016/j.jviromet.2005.01.028

it offers an advantage in the preparation of a SARS-CoV antigen because the recombinant protein of SARS-CoV can be produced without a risk of SARS-CoV-infections among laboratory workers. In the present study, we developed an IgG enzyme-linked immunosorbent assay (ELISA) in which a recombinant nucleocapsid protein (rNP) of SARS-CoV (SARS-CoV rNP) was used as an antigen, and evaluated the efficacy of the ELISA using serum samples collected from the health care workers in a hospital that was hit by a SARS-nosocomial outbreak.

2. Materials and methods

2.1. Virus

The SARS-CoV (HKU39849) used in this study was kindly supplied by Prof. J.S. Malik Peiris, Department of Microbiology, University of Hong Kong, Hong Kong Special Administrative Region.

2.2. Cells

Vero E6 cells purchased from the American Type Cell Collection (Manassas, VA) were grown in Eagle's minimum essential medium (MEM) supplemented with penicillin G and streptomycin and with 5% fetal bovine serum. The FBS was confirmed to have no inhibitory effect on the growth of SARS-CoV in cell cultures in a preliminary study. SARS-CoV was grown in Vero E6 cells cultured in MEM with penicillin G and streptomycin and with 2% fetal bovine serum.

2.3. Human serum samples

Two hundred seventy-six serum samples collected from 156 health care workers in the Hanoi French Hospital, Ho Chi Min city, Vietnam, were used (Vu et al., 2004). Serial serum samples were collected from each of the 120 subjects on different occasions. The sera were used for serological analyses after the heat-inactivation treatment at 56 °C for 30 min.

2.4. Manipulation of infectious SARS-CoV and clinical samples

All procedures that required manipulation of infectious SARS-CoV and/or non-inactivated clinical samples such as neutralizing antibody assay and authentic SARS-CoV antigen preparation were conducted in a BSL-3 laboratories in the National Institute of Infectious Diseases, Tokyo, Japan.

2.5. Recombinant baculovirus

The RNAs were extracted from SARS-CoV (HKU-39849)-infected Vero E6 cells and reverse transcribed using a random hexamer. The N gene of SARS-CoV was then amplified from the random hexamer-primed 1st strand DNAs using a forward primer (N-Bamf: 5′-GGA TCC AAT TAA AAT GTC TGA TAA TGG ACC C-3′, *Bam*HI restriction site is underlined) and a reverse primer (N-Bamr2: 5′-GGA TCC TGC CTG AGT TGA ATC AGC AG-3′, *Bam*HI restriction site is underlined). The PCR product was purified by agarose–gel electrophoresis, cloned into a pGEM-Teasy vector (Promega, Madison, USA) to generate pGEM-Teasy-N, and its sequence was confirmed to be identical to the original sequence (GenBank accession no. AY278491). The N gene insert was excised with *Bam*HI from pGEM-Teasy-N and ligated into the unique *Bam*HI site of a modified pAcYM1 baculovirus-transfer plasmid, pAc-cHis, carrying the 8His-tag at the 3′-extremity of the unique *Bam*HI site. The recombinant baculovirus, *Ac*-SARS-N-His, was then generated using the method described by Kitts et al. (1990).

2.6. Antigens

Vero E6 cells were infected with SARS-CoV for specific antigen production and also mock-infected for control antigen. Extracts of both were made similarly as follows. The authentic SARS-CoV antigen and the corresponding mock-antigen were produced as follows. Vero E6 cell were infected with SARS-CoV or the mock virus at a multiplicity of infection (moi) of 2, respectively. After incubation for 24 h, both the authentic SARS-CoV- and mock-infected Vero E6 cells were collected. The cells were washed twice with cold phosphate-buffered saline (PBS) solution and then suspended in a phosphate-buffered saline solution supplemented with 1% Nonidet-P40 (NP40). Each of the cell-suspended solutions was incubated on ice for 10 min and the cell lysates were centrifuged at 12,000 rpm for 10 min at 4 °C. The supernatant fractions prepared from the SARS-CoV-and mock-infected Vero E6 cells were inactivated by ultraviolet irradiation and were used as positive and negative antigens for IgG ELISA, respectively. The *Tn5* insect cells infected with *Ac*-SARS N-His or with *Ac*-ΔP, a baculovirus not expressing polyhedrin, were incubated for 72 h at 26 °C, respectively. Then both group of cells were washed twice with cold PBS and lysed in cold PBS containing 1% NP40 and 8 M urea. The cell lysates were centrifuged at 12,000 rpm at 4 °C for 10 min. The supernatant fractions were collected as a source of SARS-CoV rNP and negative control antigen for purification. The SARS-CoV rNP and the negative control antigen were purified using a Ni^{2+}-resin purification system (QIAGEN GmbH, Hilden, Germany), according to the manufacturer's instructions.

2.7. IgG ELISA

Authentic SARS-CoV Ag-based and the SARS-CoV rNP-based IgG ELISA were performed as described previously except for the antigen preparation (Saijo et al., 2001, 2002). The antigens were diluted with 50 mM carbonate buffer (pH 9.6) and used to coat the wells of 96-wells ELISA plates in

the present study.

2.8. Neutralizing antibody detection

The serum samples were heat-inactivated and diluted two-fold with MEM-2FBS from 1:10 to 1:320. Each test sample (60 μl by volume) was then mixed with the same volume of MEM containing SARS-CoV at an infectious dose of 100 plaque forming units per 100 μl and the mixture was incubated for 1 h at 37 °C for neutralization. After incubation, the mixtures were tested for neutralization by cytopathic effect (CPE) inhibition assay using Vero E6 cells. The neutralizing antibody titer was defined as a reciprocal of the highest dilution at which no CPE was observed.

2.9. SARS-CoV RNA amplification by a loop-mediated isothermal amplification (LAMP) method for detection of SARS-CoV

The SARS-CoV RNA genome was amplified using Loopamp SARS CoV-detection kit (Eiken Chemical, Ohtawara, Japan) as reported previously with some modifications (Hong et al., 2004). RNA was isolated from the serum samples using QIAamp viral RNA mini kit (Qiagen, Germany). Primers used in the Loopamp SARS CoV-detection kit for SARS-CoV RNA amplification were designed according to the nucleotide sequence of Replicase 1b region (GenBank accession number NC_004718). Reverse transcription-LAMP reaction was conducted in 25 μl of the reaction mixture at 62.5 °C for 45 min using the real-time turbidimeter LA200 (TERAMECS, Japan).

2.10. Statistical analysis

Sensitivity, specificity, positive predictive value (PPV) and negative predictive value (NPV) of the SARS-CoV rNP-based IgG ELISA were calculated in comparison with neutralizing antibody assay or with naive SARS-CoV antigen-based IgG ELISA (Qing et al., 2003).

Receiver operating characteristics (ROC) and two-graph-ROC (TG-ROC) curves were analyzed using Stat Flex Version 5 software (Artech Co. Ltd., Osaka, Japan) (Greiner et al., 1995; Qing et al., 2003). The relationship of the OD_{405}s in the SARS-CoV rNP-based IgG ELISA with those of the authentic viral antigen-based IgG ELISA and with the neutralizing antibody titers were evaluated by Spearman's correlation coefficient by rank using Statview software Version 5 (SAS Institute Inc., Cary, NC).

3. Results

3.1. Expression of SARS-CoV rNP

The SARS-CoV rNP was efficiently expressed in the *Tn5* insect cells infected with the recombinant *Ac*-SARS-N-His, and the purified SARS-CoV rNP was visually detected by SDS–PAGE analysis (data not shown).

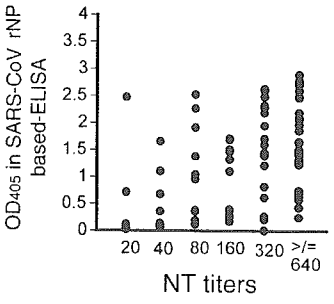

Fig. 1. Plots of the relationship between OD_{405} values at 1:100 by the SARS-CoV rNP-based IgG ELISA and neutralizing antibody titers.

3.2. Relationship of results between the IgG ELISA and neutralizing antibody assay

Of 276 serum samples, 87 showed a positive reaction in the neutralizing antibody assay. The relationship of the neutralizing antibody titers with the OD_{405} values in the SARS-CoV rNP-based IgG ELISA at a dilution level of 1:100 was evaluated using 87 neutralizing antibody-positive samples. There were significant positive correlations between the neutralizing antibody titers and the OD_{405} values in the SARS-CoV rNP-based IgG ELISA (Fig. 1, $R^2 = 0.668$, $p < 0.001$).

3.3. Efficacies of the SARS-CoV rNP-based IgG ELISA in comparison with the neutralizing antibody assay and authentic SARS-CoV-based IgG ELISA

The sensitivity, specificity, PPV and NPV, and ROC area of SARS-CoV rNP-based IgG ELISA were calculated using samples determined to be either positive or negative by neutralizing antibody assay or authentic SARS-CoV-based IgG ELISA. The relative sensitivity and specificity curves of the SARS-CoV rNP-based IgG ELISA using TG-ROC analysis are shown in Fig. 2. The sensitivity, specificity, PPV and NPV of the SARS-CoV rNP-based IgG ELISA were 92%, 92%, 83%, and 96%, respectively, when the cut-off value was set at 0.128 (the OD_{405} value at an intersectional point in Fig. 2b). The ROC area of the SARS-CoV rNP-based IgG ELISA was 0.966 when compared with either the neutralizing antibody assay. The respective values of the SARS-CoV rNP-based IgG ELISA was 94%, 94%, 87%, and 97%, respectively, compared with the naive SARS-CoV antigen-based IgG ELISA, when the cut-off value was set at 0.156 (the OD_{405} value determined in the same way as mentioned above).

3.4. Antibody responses determined by SARS-CoV rNP-based ELISA and neutralizing antibody assay in subjects with sero-conversion

Sero-conversion by neutralizing antibody assay was demonstrated in 19 of the 120 subjects, from whom serial

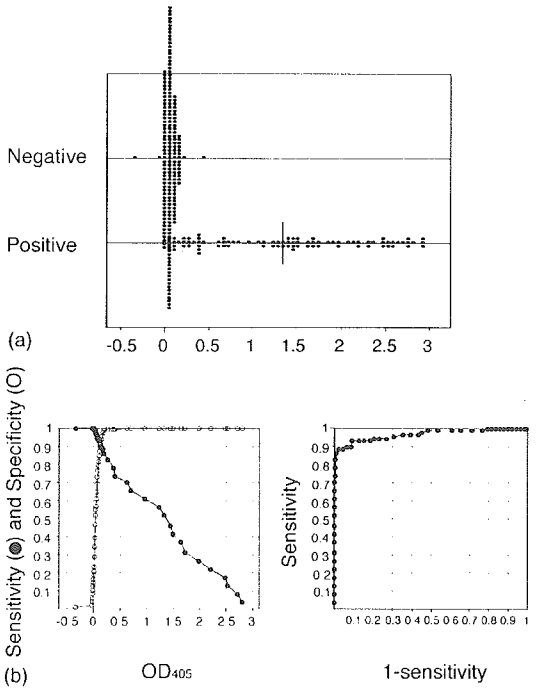

Fig. 2. Plots of (a) the OD_{405} values of the neutralizing antibody-positive and -negative samples measured by the SARS-CoV rNP-based IgG ELISA. The curves of relative sensitivity and specificity of (b) the SARS-CoV rNP-based IgG ELISA by TG-ROC analysis and (c) the ROC curve based on the neutralizing antibody assay.

serum samples were collected on different occasions. The sequential changes of OD_{405} in SARS-CoV rNP-based IgG ELISA at dilution of 1:100 and neutralizing antibody titers among the 49 serum samples collected from these 19 seroconversion-positive subjects was evaluated (Fig. 3). Each of the serum samples collected first from 17 of the 19 subjects showed a negative neutralizing antibody titer (less than 20)(black, blue or red lines in Fig. 3), while serum samples collected from the other two subjects showed a positive neutralizing antibody titers (green lines in Fig. 3). Four of the 17 neutralizing antibody-negative samples showed a positive reaction in the SARS-CoV rNP-based IgG ELISA (red lines in Fig. 3), while the other 15 showed a negative reaction in neutralizing antibody assay (black or blue lines). Only one sample that showed a positive reaction at a titer of 20 in neutralizing antibody assay showed a negative reaction in the SARS-CoV rNP-based IgG ELISA (blue line in Fig. 3).

3.5. *SARS-CoV RNA amplification and antibodies to SARS-CoV*

SARS-CoV RNA was amplified by a LAMP method in 20 serum samples collected from nine subjects. The status of antibody to SARS-CoV in these 20 serum samples was evaluated. Seven of the 20 samples showed a negative reaction in both methods of neutralizing antibody assay and SARS-CoV rNP-based IgG ELISA, two showed a negative reaction

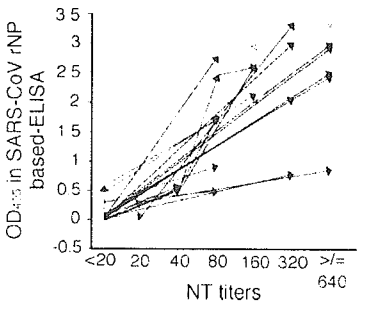

Fig. 3. Sequential change in the OD_{405} value in the SARS-CoV rNP-based IgG ELISA and neutralizing antibody titers in 19 subjects with seroconversion. The terminal positions of the tail and the cap of arrows indicate the level of OD_{405} value in the SARS-CoV rNP-based IgG ELISA at a dilution of 1:100 and neutralizing antibody titers of two serum samples collected from the same subject on different occasions. Black, red and blue arrows indicate the subjects with negative neutralizing antibody and negative antibody detectable by the SARS-CoV rNP-based IgG ELISA at the stage of the first blood collection, those with negative neutralizing antibody but positive antibody detectable by the ELISA at the same stage, and the subjects with positive neutralizing antibody but negative antibody detectable by the ELISA at the same stage, respectively. Green arrows indicate the subjects with both positive neutralizing antibody and positive antibody detectable by the ELISA at the same stage.

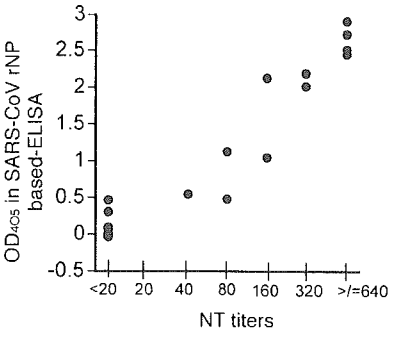

Fig. 4. Plots of the relationship between OD_{405} values at 1:100 by the SARS-CoV rNP-based IgG ELISA and neutralizing antibody titers in the 20 serum samples with positive SARS-CoV genome.

in neutralizing antibody assay but a positive reaction in the ELISA, while the other 11 samples showed a positive reaction in both assays (Fig. 4).

4. Discussion

SARS-CoV was revealed to have a 30 kb long viral genome, containing 14 potential open reading frames (ORFs) (8). The sequence of SARS-CoV reveals the presence of ORFs for four structural proteins; i.e., the spike, membrane, envelope and nucleocapsid protein. Among these structural proteins, we selected the nucleocapsid protein, SARS-CoV rNP, as an antigen. Tan et al. recently reported that antibodies to the nucleocapsid and spike proteins of SARS-CoV were demonstrated in 100% of convalescent-phase patients, while antibodies to U274, a protein unique to SASR-CoV,

was demonstrated in 73% of the patients (Tan et al., 2004), indicating that SARS-CoV rNP was the best choice as an antigen among the SARS-CoV structural proteins. Similar results were reported by Woo et al. (2004).

This study was performed using a relatively large panel of serum samples collected from health care workers from a Vietnamese hospital. We developed a recombinant SARS-CoV nucleocapsid protein-based IgG ELISA and confirmed that the ELISA had a higher than 90% sensitivity and specificity in detecting IgG antibodies to SARS-CoV compared with neutralizing antibody assay, the gold standard method, and with the authentic SARS-CoV Ag-based IgG ELISA (Fig. 2). There was a positive correlation between the OD_{405} values in the SARS-CoV rNP-based IgG ELISA and the neutralizing antibody titers (Fig. 1). Furthermore, sequential change in OD_{405} in the SARS-CoV rNP-based IgG ELISA and neutralizing antibody titers in 19 subjects, in whom seroconversion was demonstrated, was evaluated (Fig. 3). Four of the 19 had already had antibody to SARS-CoV rNP detectable by SARS-CoV rNP-based IgG ELISA, although at this stage they had not yet had a neutralizing antibody equal to or over 20. On the other hand, only one serum sample that showed a positive reaction in neutralizing antibody assay at a titer of 20 showed a negative reaction in the SARS-CoV rNP-based IgG ELISA (Fig. 3). These results suggest that this SARS-CoV rNP-based IgG ELISA is as sensitive as the neutralizing antibody assay. Therefore, it can be concluded that the newly developed SARS-CoV rNP-based IgG ELISA is useful for the serological diagnosis of and seroepidemiological study on SARS-CoV infections.

The SARS-CoV rNP-based IgG ELISA was evaluated for efficacy in detection of specific antibody to SARS-CoV in comparison with neutralizing antibody assay in the present study. There have been several reports on the SARS-CoV rNP-based serological diagnostic system (Chan et al., 2005; Guan et al., 2004; Lin et al., 2003; Shi et al., 2003; Woo et al., 2004). Lin et al. (2003) first reported that SARS-CoV rNP would be one of the candidates for the antigen to detect SARS-CoV antibodies. They confirmed that three of the nine serum samples collected from the patients clinically diagnosed as having SARS showed a positive reaction in SARS-CoV rNP-based Western blotting. The SARS-CoV rNP was then expressed in an *E. coli* system and used as antigen in an antigen-capturing ELISA. It was reported that the antigen-capturing ELISA had high specificity of about 98%, though the sensitivity was not evaluated in the study (Shi et al., 2003). Recently, Guan et al. also reported the efficacy of the recombinant protein of SARS-CoV-based IgG ELISA in diagnosis of SARS (Guan et al., 2004). The SARS-CoV rNP was also expressed in *E. coli* transformed with an expression vector. However, these systems were not compared with the neutralizing antibody assay that is considered to be a gold standard.

The indices of sensitivity, specificity, PPV and NPV of our ELISA were relatively lower than those of the previous reports (Guan et al., 2004; Shi et al., 2003). These differences might be due to differences in the nature of the sera used in the study or due to the methods for the evaluation, or due to the both factors.

The status of antibody to SARS-CoV in the SARS-CoV genome-positive serum samples was evaluated. It was revealed that SARS-CoV genome is still present at a stage of IgG responses in some cases of SARS (Fig. 4). The results indicate that handling of blood collected from patients with SARS must be handled very carefully even if the patients were in a recovery phase with IgG responses. Furthermore, SARS-CoV amplification by a sensitive assay such as LAMP method should be carried out as a diagnostic tool, even when patients with SARS were in a stage of IgG responses.

In summary, a SARS-CoV rNP-based IgG ELISA with high sensitivity and specificity was developed. The advantage of the SARS-CoV rNP-based IgG ELISA is that the antigen can be prepared without the risk of infection.

Acknowledgements

We thank Prof. J.S. Malik Peiris, Department of Microbiology, University of Hong Kong, for providing us with the SARS-CoV (HKU-39849). We also thank Ms. M. Ogata, Department of Virology 1, National Institute of Infectious Diseases, Tokyo, Japan, for her technical assistance. This work is supported by grants-in-aid from the Ministry of Health, Labor and Welfare of Japan.

References

CDC, 2003. Update: outbreak of severe acute respiratory syndrome-worldwide, 2003. MMWR Morb. Mortal Wkly. Rep. 52, 241–248.

Chan, P.K., Liu, E.Y., Leung, D.T., Cheung, J.L., Ma, C.H., Tam, F.C., Hui, M., Tam, J.S., Lim, P.L., 2005. Evaluation of a recombinant nucleocapsid protein-based assay for anti-SARS-CoV IgG detection. J. Med. Virol. 75, 181–184.

Greiner, M., Sohr, D., Gobel, P., 1995. A modified ROC analysis for the selection of cut-off values and the definition of intermediate results of serodiagnostic tests. J. Immunol. Methods 185, 123–132.

Guan, M., Chen, H.Y., Foo, S.Y., Tan, Y.J., Goh, P.Y., Wee, S.H., 2004. Recombinant protein-based enzyme-linked immunosorbent assay and immunochromatographic tests for detection of immunoglobulin G antibodies to severe acute respiratory syndrome (SARS) coronavirus in SARS patients. Clin. Diagn. Lab. Immunol. 11, 287–291.

Hong, T.C., Mai, Q.L., Cuong, D.V., Parida, M., Minekawa, H., Notomi, T., Hasebe, F., Morita, K., 2004. Development and evaluation of a novel loop-mediated isothermal amplification method for rapid detection of severe acute respiratory syndrome coronavirus. J Clin Microbiol 42, 1956–1961.

Kitts, P.A., Ayres, M.D., Possee, R.D., 1990. Linearization of baculovirus DNA enhances the recovery of recombinant virus expression vectors. Nucl. Acids Res. 18, 5667–5672.

Lee, N., Hui, D., Wu, A., Chan, P., Cameron, P., Joynt, G.M., Ahuja, A., Yung, M.Y., Leung, C.B., To, K.F., Lui, S.F., Szeto, C.C., Chung, S., Sung, J.J., 2003. A major outbreak of severe acute respiratory syndrome in Hong Kong. N. Engl. J. Med. 348, 1986–1994.

Lin, Y., Shen, X., Yang, R.F., Li, Y.X., Ji, Y.Y., He, Y.Y., Shi, M.D., Lu, W., Shi, T.L., Wang, J., Wang, H.X., Jiang, H.L., Shen, J.H., Xie, Y.H., Wang, Y., Pei, G., Shen, B.F., Wu, J.R., Sun, B., 2003. Identification of an epitope of SARS-coronavirus nucleocapsid protein. Cell. Res. 13, 141–145.

Poutanen, S.M., Low, D.E., Henry, B., Finkelstein, S., Rose, D., Green, K., Tellier, R., Draker, R., Adachi, D., Ayers, M., Chan, A.K., Skowronski, D.M., Salit, I., Simor, A.E., Slutsky, A.S., Doyle, P.W., Krajden, M., Petric, M., Brunham, R.C., McGeer, A.J., and National Microbiology Laboratory, C.C.S.A.R.S.S.T, 2003. Identification of severe acute respiratory syndrome in Canada. N. Engl. J. Med. 348, 1995–2005.

Qing, T., Saijo, M., Lei, H., Niikura, M., Maeda, A., Ikegami, T., Xinjung, W., Kurane, I., Morikawa, S., 2003. Detection of immunoglobulin G to Crimean-Congo hemorrhagic fever virus in sheep sera by recombinant nucleoprotein-based enzyme-linked immunosorbent and immunofluorescence assays. J. Virol. Methods 108, 111–116.

Saijo, M., Niikura, M., Morikawa, S., Ksiazek, T.G., Meyer, R.F., Peters, C.J., Kurane, I., 2001. Enzyme-linked immunosorbent assays for detection of antibodies to Ebola and Marburg viruses using recombinant nucleoproteins. J. Clin. Microbiol. 39, 1–7.

Saijo, M., Qing, T., Niikura, M., Maeda, A., Ikegami, T., Prehaud, C., Kurane, I., Morikawa, S., 2002. Recombinant nucleoprotein-based enzyme-linked immunosorbent assay for detection of immunoglobulin G antibodies to Crimean-Congo hemorrhagic fever virus. J. Clin. Microbiol. 40, 1587–1591.

Shi, Y., Yi, Y., Li, P., Kuang, T., Li, L., Dong, M., Ma, Q., Cao, C., 2003. Diagnosis of severe acute respiratory syndrome (SARS) by detection of SARS coronavirus nucleocapsid antibodies in an antigen-capturing enzyme-linked immunosorbent assay. J. Clin. Microbiol. 41, 5781–5782.

Tan, Y.J., Goh, P.Y., Fielding, B.C., Shen, S., Chou, C.F., Fu, J.L., Leong, H.N., Leo, Y.S., Ooi, E.E., Ling, A.E., Lim, S.G., Hong, W., 2004. Profiles of antibody responses against severe acute respiratory syndrome coronavirus recombinant proteins and their potential use as diagnostic markers. Clin. Diagn. Lab. Immunol. 11, 362–371.

Tsang, K.W., Ho, P.L., Ooi, G.C., Yee, W.K., Wang, T., Chan-Yeung, M., Lam, W.K., Seto, W.H., Yam, L.Y., Cheung, T.M., Wong, P.C., Lam, B., Ip, M.S., Chan, J., Yuen, K.Y., Lai, K.N., 2003. A cluster of cases of severe acute respiratory syndrome in Hong Kong. N. Engl. J. Med. 348, 1977–1985.

Vu, H.T., Leitmeyer, K.C., Le, D.H., Miller, M.J., Nguyen, Q.H., Uyeki, T.M., Reynolds, M.G., Aagesen, J., Nicholson, K.G., Vu, Q.H., Bach, H.A., Plan, A.J., 2003. Clinical description of a completed outbreak of SARS in Vietnam February–May. Emerg. Infect. Dis. 10, 334–338.

WHO, 2003. Summary of probable SARS cases with onset of illness from 1 November 2002 to 31 July 2003.

Woo, P.C., Lau, S.K., Tsoi, H.W., Chan, K.H., Wong, B.H., Che, X.Y., Tam, V.K., Tam, S.C., Cheng, V.C., Hung, I.F., Wong, S.S., Zheng, B.J., Guan, Y., Yuen, K.Y., 2004. Relative rates of non-pneumonic SARS coronavirus infection and SARS coronavirus pneumonia. Lancet 363, 841–845.

Journal of Medical Virology 76:111–118 (2005)

Characterization of Monoclonal Antibodies to Marburg Virus Nucleoprotein (NP) That can be Used for NP-Capture Enzyme-Linked Immunosorbent Assay

Masayuki Saijo,[1]* Masahiro Niikura,[1] Akihiko Maeda,[1] Tetsutaro Sata,[2] Takeshi Kurata,[2] Ichiro Kurane,[1] and Shigeru Morikawa[1]

[1]*Special Pathogens Laboratory, Department of Virology 1, National Institute of Infectious Diseases, Musashimurayama, Tokyo, Japan*

[2]*Department of Infectious Disease Pathology, National Institute of Infectious Diseases, Musashimurayama, Tokyo, Japan*

After the first documented outbreak of Marburg hemorrhagic fever identified in Europe in 1967, several sporadic cases and an outbreak of Marburg hemorrhagic fever have been reported in Africa. In order to establish a diagnostic system for Marburg hemorrhagic fever by the detection of Marburg virus nucleoprotein, monoclonal antibodies to the recombinant nucleoprotein were produced. Two clones of monoclonal antibodies, MAb2A7 and MAb2H6, were efficacious in the antigen-capture enzyme-linked immunosorbent assay (ELISA). At least 40 ng/ml of the recombinant nucleoprotein of Marburg virus was detected by the antigen-capture ELISA format. The epitope of the monoclonal antibody (MAb2A7) was located in the carboxy-terminus of nucleoprotein from amino acid position 634 to 647, while that of the MAb2H6 was located on the extreme region of the carboxy-terminus of the Marburg virus nucleoprotein (amino acid position 643–695). These monoclonal antibodies strongly interacted with the conformational epitopes on the carboxy-terminus of the nucleoprotein. Furthermore, these two monoclonal antibodies were reacted with the authentic Marburg virus antigens by indirect immunofluorescence assay. These data suggest that the Marburg virus nucleoprotein-capture ELISA system using the monoclonal antibodies is a promising technique for rapid diagnosis of Marburg hemorrhagic fever. ***J. Med. Virol. 76:111–118, 2005.*** © 2005 Wiley-Liss, Inc.

KEY WORDS: Marburg virus; antigen-capture ELISA; monoclonal antibody; diagnosis

INTRODUCTION

Marburg virus (MBGV) infections cause one of the most severe forms of hemorrhagic fevers with a high mortality rate [Feldmann et al., 1996; Anonymous, 1999; Bausch et al., 2003]. MBGV belongs to the genus Marburg-like virus, family Filoviridae. Ebola viruses (EBOVs), which belong to genus Ebola-like virus, family Filoviridae, also cause Ebola hemorrhagic fever with a high mortality rate [Peters and LeDuc, 1999]. The first documented outbreak of Marburg hemorrhagic fever occurred in the former West Germany and the former Yugoslavia in 1967 [Martini et al., 1968]. The outbreak occurred among scientists and technicians who had handled monkeys, or their tissues, imported from Uganda [Martini et al., 1968]. Thirty-two patients were affected and seven died in the outbreak. After the first documented outbreak, three sporadic cases of Marburg hemorrhagic fever were reported in Zimbabwe (1975) and Kenya (1980 and 1987), resulting in the diagnosis of six patients with Marburg hemorrhagic fever [Smith et al., 1982; Conrad et al., 1987; Feldmann et al., 1996; Johnson et al., 1996]. Human to human transmission of Marburg hemorrhagic fever was documented in an outbreak in South Africa after patients with Marburg hemorrhagic fever had been transferred there from Zimbabwe [Gear et al., 1975]. Three of the six patients in

Grant sponsor: Ministry of Health, Labor, and Welfare of Japan.

*Correspondence to: Masayuki Saijo, MD, PhD, Special Pathogens Laboratory, Department of Virology 1, National Institute of Infectious Diseases, 4-7-1 Gakuen, Musashimurayama, Tokyo 208-0011, Japan. E-mail: msaijo@nih.go.jp

Accepted 17 January 2005

DOI 10.1002/jmv.20332

Published online in Wiley InterScience (www.interscience.wiley.com)

these sporadic outbreaks died. From 1998 to 1999, there was a large outbreak of Marburg hemorrhagic fever in the Democratic Republic of Congo, former Zaire [Bausch et al., 2003]. More than 100 patients with Marburg hemorrhagic fever were reported in that outbreak and the mortality rate was more than 50%.

Marburg hemorrhagic fever should be confirmed by virus isolation, detection of virus antigen and/or virus genome, or by detection of specific immunoglobulin M (IgM) and immunoglobulin G (IgG) using samples from patients. Virus isolation, electron microscopic examination, and reverse-transcription polymerase chain reaction (RT-PCR) are used for the diagnosis of Marburg virus infection [Ksiazek et al., 1999; Sanchez et al., 1999]. Although antigen-capture ELISA systems have been used for the diagnosis of Ebola hemorrhagic fever [Ksiazek et al., 1999], no antigen-capture ELISA for Marburg virus has yet been used for confirmation of infection.

In the present study, monoclonal antibodies to the recombinant nucleoprotein (rNP) of MBGV were generated and an antigen-capture ELISA using these monoclonal antibodies was developed. These monoclonal antibodies efficacious were characterized.

MATERIALS AND METHODS

Cell Culture

Hybridomas and their parental cell line, P3/Ag568, were maintained in PRMI 1640 (Invitrogen life technologies, Carlsbad, CA) supplemented with 10% fetal bovine serum (FBS), nonessential amino acids (Invitrogen), and antibiotics (streptomycin and penicillin G, Invitrogen). Hypoxanthine-aminopterin-thymidine supplement (Invitrogen) was added to the medium for selection of hybridomas, as recommended by the supplier. High five (Tn5) insect cells were maintained in TC100 (Invitrogen) supplemented with 10% FBS, 2% tryptose phosphate broth (Difco, Detroit, MI), and kanamycin (Invitrogen).

Authentic MBGV Antigen

Radiation-inactivated and acetone-fixed authentic MBGV (the Musoke strain)-infected Vero E6 cells spotted on slides for immunofluorescence testing were kindly supplied to T.K. in 1987 by Dr. J.B. McCormick, former chief of the Special Pathogens Branch, Division of Viral and Rickettsial Diseases, Centers for Disease Control and Prevention, Atlanta, GA.

rNP of MBGV

A full-length rNP of MBGV tagged with a 6× histidine at the amino-terminus was expressed using a baculovirus system [Saijo et al., 2001]. The DNA corresponding to each truncated NP fragment was amplified with the primers from a cDNA clone of NP of MBG provided by H.-D. Klenk, Philipps-University, Marburg, Germany. The full-length rNP of MBGV consisted of 695 amino acid residues. The truncated rNP fragments of the carboxy-terminal region of MBGV (MBG-NP/C-half, amino acid positions 341–695) was also expressed in an *Escherichia coli* (*E. coli*) system as a fusion protein with glutathione *S*-transferase (GST) as described previously [Saijo et al., 2001]. Smaller fragments of the rNP in the extreme carboxy-terminus (MBG-NP8, amino acid position 595–695) were also expressed as a form of GST-fusion protein at the amino-terminal portion in the *E. coli* system transformed with the respective pGEX-2T vector (Amersham Biosciences Corp., Piscataway, NJ) inserted with the corresponding DNA of the MBGV nucleoprotein. The data on the primers used for making the corresponding DNA regions are shown in Table I. The nucleotide sequence of the inserted DNAs was determined to exclude PCR errors.

The full-length rNP of MBGV was purified with the N^{2+}-resin purification system (Qiangen GmbH, Hilden, Germany). The GST-MBG-NP/C-half was also purified with glutathione Sephalose 4B (Amersham Biosciences Corp.). The protein concentration of the purified rNP of MBGV was measured by the Bradford method using

TABLE I. Primers Used in the Present Study

Sequence[a]	Name	Nucleotide position[b]	Direction
GGTGATTGATCAGAACCTATAAGATC	MBG-NP 8F	1771–1796	Forward
CAGGAATGATCAAGGATGAGGGAAGCC	MN8/2F	1819–1845	Forward
CTCTGGAATTCATGTTTGCAGAAGATCA	MN8/2R	1944–1971	Reverse
TTCACATGATCAGAGGATAATCAGCAG	MN8/3F	1864–1890	Forward
CAGGAATTCAGTATTCCTCAACGAGGGC	MN8/3R	1984–2011	Reverse
AAGAAGTGATCAACTTTCCTTTATC	MN8/4F	1915–1939	Forward
TTCATGAATTCACATGTCGGGCCAATC	MN8/4R	2035–2061	Reverse
GCTGAATTCTCTGGACTACAAGTTC	MBG-NP 8R	2079–2103	Reverse
CAGGGATCCTGGCCACAAAGAGTG	M8/2F-6	1885–1908	Forward
AATGGATCCCAAAGAGTGGTGAC	M8/2F-8	1891–1913	Forward
CCAGGATCCGTGGTGACAAAGAAG	N8/2F-10	1897–1920	Forward
GCAGAAGAATTCAAGGATAAAGGAAAG	M8/3R-6	1928–1954	Reverse
GATCATGAATTCAAAGGAAAGTTCTAC	M8/3R-8	1922–1948	Reverse
TAGGAGAATTCAAAGTTCTACCCTTC	M8/3R-10	1917–1942	Reverse

[a]Restriction sites are underlined.
[b]Nucleotide position is counted from the initiation ATG codon of the nucleotide gene of Marburg virus (GemBack Accession No. X68495).

Protein Assay™ (Bio-Rad Laboratories, Hercules, CA) according to the manufacturer's instructions.

rNP of EBOV

The full-length rNP of Zaire Ebola virus was expressed by the baculovirus system and purified as described previously [Saijo et al., 2001].

Establishment of Monoclonal Antibodies

BALB/c mice were immunized three times with the purified GST-MBG-NP/C-half. Spleen cells were obtained 3 days after the last immunization and fused with P3/Ag568 cells using polyethylene glycol (Invitrogen). The culture supernatants of the hybridoma cells were screened by ELISA with purified GST-MBG-NP/C-half as an antigen. Monoclonal antibodies were purified from the culture supernatant with an MAb Trap GII antibody purification kit (Amersham Biosciences Corp.) according to the manufacturer's instructions. The isotypes of the monoclonal antibodies were determined with a Mouse Monoclonal Antibody Isotyping Kit (Invitrogen). The concentration of each purified monoclonal antibody was also determined by the Bradford method using Protein Assay (Bio-Rad Laboratories) according to the manufacturer's instructions.

Polyclonal and Monoclonal Antibodies

The polyclonal antibody was induced in rabbits by immunization with the purified rNP of MBGV expressed in the baculovirus system [Saijo et al., 2001]. Rabbit and mouse sera collected before immunization were used as controls.

A monoclonal antibody to rNP of EBOV (3-3D), which is efficacious in the EBOV nucleoprotein-capture ELISA, was used [Niikura et al., 2001].

Antigen-Capture ELISA

Purified monoclonal antibody was coated on microwell immunoplates (Falcon, Becton Dickinson Labware, Franklin Lakes, NJ) at >100 ng/well in 100 μl of PBS at 4°C overnight, followed by blocking with PBS containing 5% nonfat milk and 0.05% Tween-20 (PBST-M) for 1 hr at room temperature (RT). After the plates were washed with phosphate-buffered saline solution (PBS) containing 0.05% Tween-20 (PBST), 100 μl of samples containing serially diluted rNP of MBGV were added and the plates were incubated for 1 hr at 37°C. The plates were then washed with PBST, and 100 μl of rabbit polyclonal antibody raised against rNP of MBGV diluted 1:500 with PBST-M was added to each well. After 1 hr incubation at 37°C, the plates were washed with PBST and horseradish peroxidase (HRPO)-conjugated goat anti-rabbit IgG (Zymed Laboratories, Inc., South San Francisco, CA) was added. The plates were incubated for 1 hr at RT. After another extensive wash with PBST, 100 μl of ABTS substrate solution [4 mM 2,2-azino-di[3-ethylbenzthiazolinesulfate(6)] solution; 2.5 mM hydrogen superoxygenphosphate (pH 4.2)] (Roche Diagnostics, Mannheim, Germany) was added and the optical density (OD) was measured at a wavelength of 405 nm with a reference wavelength 490 nm after 30 min of incubation at 37°C. As a negative control, mock antigen-inoculated wells were tested. The adjusted OD values (OD_{405}) were calculated by subtracting the OD of the negative control well from the corresponding OD values.

Western Blotting

The monoclonal antibodies were tested for reactivity to the recombinant rNP fragments by Western blotting. Briefly, the expressed rNP fragment series were separated by sodium dodecyl sulfate–polyacrylamide gel electrophoresis (SDS–PAGE) and the separated proteins were transblotted to the nitrocellulose membrane (Millipore, Bedford, MA). The monoclonal antibodies that reacted with the blots were detected with HRPO-conjugated gout anti-mouse IgG (Zymed) and peroxidase substrate (POD substrate, Wako Pure Chimeical, Tokyo, Japan). The monoclonal antibody to GST produced in our laboratory was also used. The SDS–PAGE gels were prepared in the same way as those for Western blotting and were stained by Coomassie staining solution for visualization.

Indirect Immunofluorescence Assay (IFA)

The authentic MBGV for IFA were reacted with each of the monoclonal antibodies or control mouse serum at 37°C for 1 hr in humidified conditions. Slides were then washed with PBS and the antigens were reacted with fluorescein isothiocyanate (FITC)-conjugated goat anti-mouse IgG antibody (Zymed). As a control, the antigens were simultaneously reacted with either the polyclonal antibody to the rNP of MBGV or a control rabbit serum at 37°C for 1 hr in a humidified condition. The slides were washed with PBS and the antigens were reacted with FITC-conjugated goat anti-rabbit IgG antibody (Zymed). After washing with PBS, the fluorescein-signal was observed under an immunofluorescent microscope (Carl Zeiss, Oberkochen, Germany).

RESULTS

Generation of Monoclonal Antibodies

Five hybridoma clones secreting IgG antibodies to GST-MBG-rNP/C-half were produced. The secreted monoclonal antibodies were purified and tested for reactivity to the rNP of MBGV in IgG-ELISA. Four monoclonal antibodies reacted with the rNP of MBGV in IgG-ELISA. Two of these four monoclonal antibodies secreted from the hybridoma clones, 2A7 and 2H6, could be used in the antigen-capture ELISA format. These two monoclonal antibodies were designated as MAb2A7 and MAb2H6, respectively. The isotype of MAb2A7 and MAb2H6 was IgG1.

Antigen-Capture ELISA Using the Monoclonal Antibodies

The antigen-capture ELISA with MAb2A7 or MAb2H6 detected at least 40 ng/ml of the purified rNP of Marburg virus, while the ELISA with mock-antibody (PBS) showed a negative reaction (Fig. 1). Furthermore, the ELISA did not react with negative control samples that did not contain rNP of MBGV.

Definition of Epitopes Recognized by the Monoclonal Antibodies

The MAb2A7 and MAb2H6 reacted with both GST-MBG-NP/C-half and GST-MBG-NP8 in Western blotting. Smaller fragments of the MBG-NP8 region were expressed and the reactivity of these monoclonal antibodies to these fragments was analyzed (Fig. 2).

The MAb2A7 reacted with all the fragments that contained the polypeptide of amino acid residues from amino acid position 626 to 653 (Fig. 2). Truncated polypeptides of this region were further designed and expressed as shown in Fig. 3. Reactivity of the monoclonal MAb2A7 to these fragments was evaluated (Fig. 3). The MAb2A7 reacted with the polypeptide, "WPQRVVTKKGRTFL (amino acid positions 632–645)" (Fig. 3). Although the epitope of the MAb2A7 was located in this region, MAb2A7 reacted with the MBG-NP8/1-5 (amino acid positions 595–695) more strongly than with the smaller fragments (Fig. 2), indicating that the reactivity of MAb2A7 with the nucleoprotein of MBGV was influenced by conformational and structural properties.

The MAb2H6 strongly reacted with the truncated polypeptides containing the extreme carboxy-terminal region and which were larger than the polypeptides mentioned above (Fig. 4). The smallest polypeptide to react with MAb2H6 was that consisting of amino acid residues (amino acid positions 643–695). MAb2H6 did not reacted with any of the polypeptides lacking the extreme carboxy-terminal region (amino acid positions 584–695) (Fig. 4). These results indicate that MAb2H6 reacted with the conformational epitope composed of the extreme carboxy-terminal region.

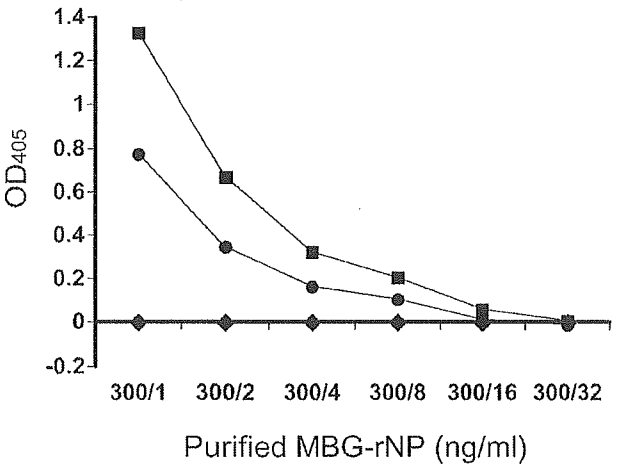

Fig. 1. Reactivity of each monoclonal antibody in the antigen-capture enzyme-linked immunosorbent assay (ELISA) format. Purified monoclonal antibodies (■, MAb2A7; ●, MAb2H6; ◆, mock) were coated onto the microplates as described in the text, and their ability to capture the rNP of Marburg virus (MBGV) was examined at various concentrations of MBGV rNP in the antigen-capture format.

Reactivity of the Monoclonal Antibodies to Authentic MBGV Antigen in IFA

MAb2A7 and MAb2H6 both reacted with the authentic MBGV antigens by the IFA test as well as the rabbit serum raised to rNP of MBGV. Negative control mouse and rabbit sera did not react with the authentic antigens (Fig. 5).

Reactivity of the Monoclonal Antibodies to rNP of EBOV

Neither of MAb2A7 and MAb2H6 reacted with the rNP of EBOV by both Western blotting and the antigen-detection ELISA, while MAb3-3D reacted with rNP of EBOV (Fig. 6). Both MAb2A7 and MAb2H6 reacted with rNP of MBGV by both the Western blotting and the antigen-detection ELISA, but MAb3-3D did not (Fig. 6).

DISCUSSION

Detection of MBGV antigen and amplification of viral genome of MBGV is necessary for rapid diagnosis of Marburg hemorrhagic fever. The application of RT-PCR and TaqMan PCR to MBGV genome amplification has been suggested [Sanchez et al., 1999; Drosten et al., 2002]. Although, serological diagnosis is also useful for the diagnosis of Marburg hemorrhagic fever, serum samples collected at both acute and convalescent phases are required, suggesting that serological diagnosis may not be suitable in certain areas and that it may not be applied in fatal cases without antibody responses. Therefore, a novel antigen-capture ELISA has been developed in the present study.

Two monoclonal antibodies (MAb2A7 and MAb2H6) developed in the study reacted with the authentic MBGV antigens by IFA (Fig. 5). At least 40 ng/ml of rNP of MBGV was detected in the MBGV nucleoprotein-capture ELISA using these monoclonal antibodies (Fig. 1). Unfortunately, the efficacy of the developed antigen-capture ELISA has not been validated using clinical samples, because clinical samples from patients with Marburg hemorrhagic fever at an acute phase were not available. It is generally accepted that antigen-capture ELISA is useful for the detection of viral antigens in blood and/or other organ tissue specimens collected not only from surviving patients but also from patients in whom the infection was fatal. The present study suggests that the antigen-capture ELISA using the unique monoclonal antibodies is a useful tool for diagnosis.

The nucleoprotein-detection ELISA systems for Zaire Ebola and Reston Ebola viruses were developed by

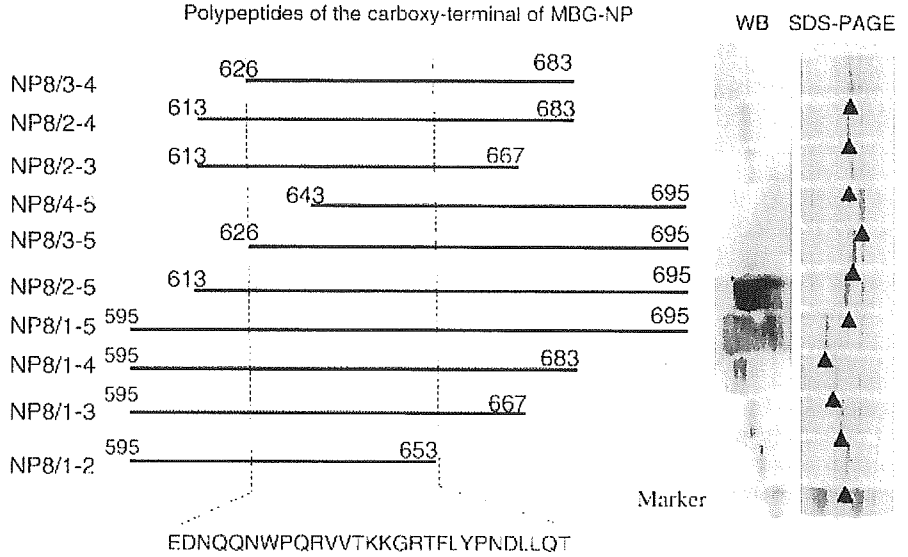

Fig. 2. Schematic representation of the truncated polypeptides (**left part**), expression levels of these polypeptides determined by sodium dodecyl sulfate–polyacrylamide gel electrophoresis (SDS–PAGE) analysis (right part, SDS–PAGE), and reactivity of MAb2A7 to these polypeptides in Western blotting (WB) (**right part**, WB). The numbers shown for each schematic polypeptide indicate the amino acid positions of the MBGV nucleoprotein.

previous studies [Niikura et al., 2001; Ikegami et al., 2003]. Interestingly, the monoclonal antibodies, which could be used as antigen-capture antibodies in the antigen-capture ELISA systems, reacted with the carboxy-terminal regions of Ebola virus nucleoproteins. The monoclonal antibodies in the present study also reacted with a similar region of the nucleoprotein of MBGV. Although data are not shown here, none of monoclonal antibodies to nucleoproteins of Ebola and Marburg viruses, which reacted with regions other than the approximately 100 amino acid residues at the carboxy-terminal region, were found to be useful as antigen-capture antibodies in the antigen-capture ELISA. Thus, it is likely that the monoclonal antibodies to nucleoproteins of filoviruses useful in antigen-capture ELISA systems react with the carboxy-terminal region of the nucleoproteins.

The symptoms due to MBGV infections in humans and non-human primates are indistinguishable from those due to EBOV infections. Therefore, it was considered that reactivity of the monoclonal antibodies to the nucleoprotein of EBOV should be examined. It was confirmed that neither of monoclonal antibodies, 2A7 and 2H6, cross-reacted with nucleoprotein of EBOV

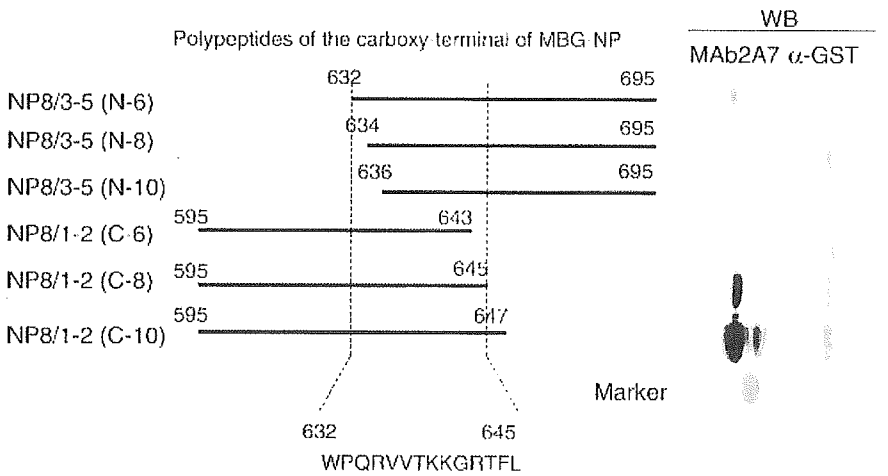

Fig. 3. Schematic representation of the truncated polypeptides (**left part**), and reactivity of MAb2A7 and anti-glutathione *S*-transferase (GST) monoclonal antibody to these polypeptides in WB. The numbers shown for each schematic polypeptide indicate the amino acid positions of the MBGV nucleoprotein.

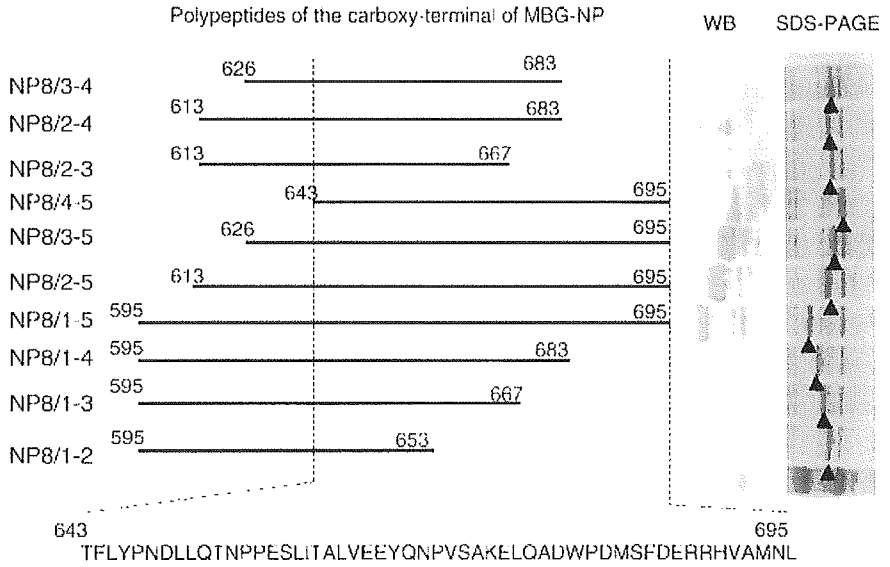

Fig. 4. Schematic representation of the truncated polypeptides (**left part**), expression levels of these polypeptides determined by SDS–PAGE analysis (right part, SDS–PAGE), and reactivity of MAb2H6 to these polypeptides in Western blotting (**right part**, WB). The numbers shown for each schematic polypeptide indicate the amino acid positions of the MBGV nucleoprotein.

(Fig. 6), indicating that the newly developed MBGV nucleoprotein-detection ELISA was specific for MBGV infections.

The amino acid sequence of the polypeptide recognized by MAb2A7 was conserved among Marburg virus isolates so far deposited in the GenBank, and there is no significant diversity in the amino acid sequences of the carboxy-terminal regions among Marburg virus isolates (http://www.ncbi.nlm.nih.gov/entrez/query.fcgi?db=Protein, Accession nos. AAR85460, AAR85453,

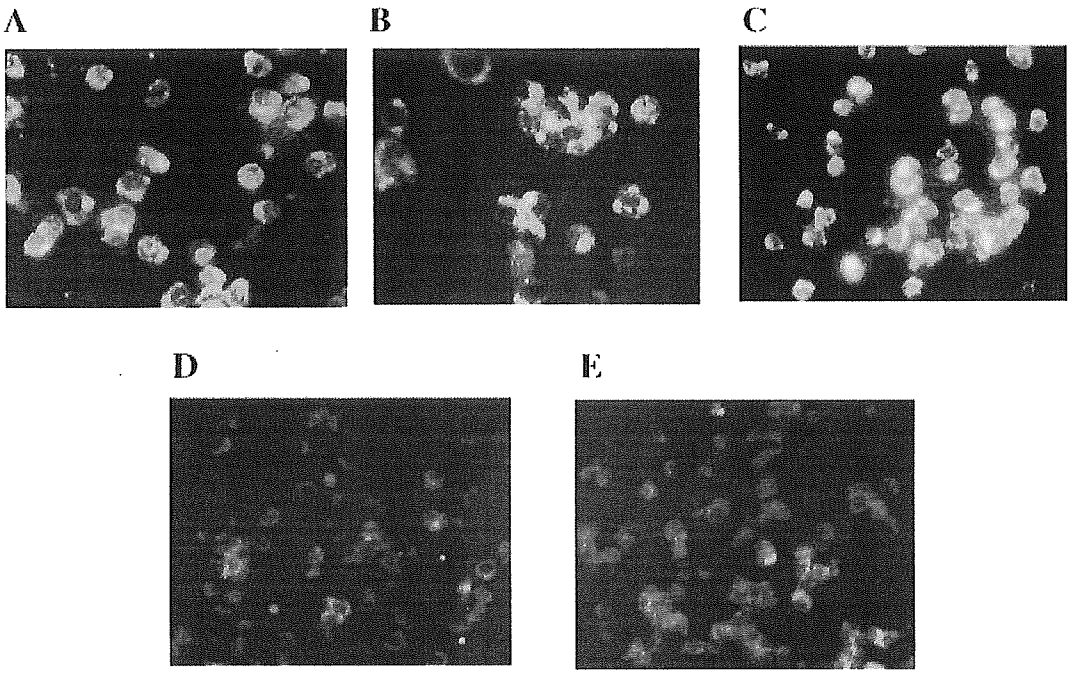

Fig. 5. Reactivity of MAb2A7 (**A**), MAb2H6 (**B**), anti-MBGV rNP rabbit serum (**C**), negative control mouse serum (**D**), and rabbit serum (**E**) to authentic MBGV antigens in Vero E6 cells in the immunofluorescence assay.

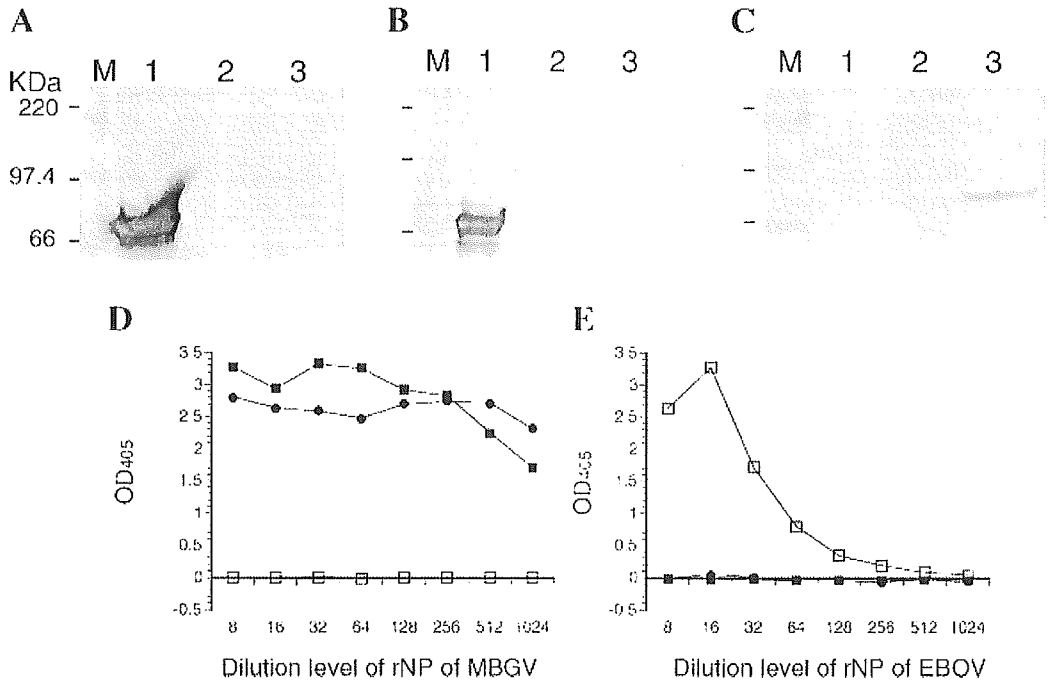

Fig. 6. Reactivity of the monoclonal antibodies to rNPs of MBGV and EBOV. Reactivity of MAb2A7 (**A**), MAb2H6 (**B**), and MAb3-3D (**C**) to MBGV rNP and EBOV rNP was examined in Western blotting. Lanes "M," "1," "2," and "3" indicate the lanes blotted with markers, GST-tagged MBG-NP/C-half, negative control antigen prepared from *Tn5* insect cells infected with the recombinant baculovirus without expression of foreign genes, and His-tagged rNP of EBOV, respectively [Saijo et al., 2001]. Reactivity of these monoclonal antibodies to the rNPs of MBGV (**D**) and EBOV (**E**) was also examined in the antigen-capture ELISA using MAb2A7 (■), MAb2H6 (●), or MAb3-3D (□).

NP_042025, AAQ55255, S44049, VHIWMV, P35263, 2110212A, P27588, CAA78114, CAA82536, AAA46563). Therefore, it is quite likely that the newly developed antigen-capture ELISA system for MBGV is useful for detecting most MBGV isolates, although further study is needed.

In conclusion, an MBGV nucleoprotein-detection ELISA system using unique monoclonal antibodies was developed, and the monoclonal antibodies useful for detecting nucleoprotein of the MBGV in the system were characterized. The combined use of the MBGV nucleoprotein-capture ELISA in the present study with the EBOV nucleoprotein-detection ELISA developed in a previous study [Niikura et al., 2001; Ikegami et al., 2003] may be useful for the diagnosis of viral hemorrhagic fevers due to filovirus infections.

ACKNOWLEDGMENTS

The study was performed with the approval of the ethical committee for animal experiments established in the National Institute of Infectious Diseases, Tokyo, Japan. We thank Prof. H.D. Klenk, Institute of Virology, Philipps-University, Marburg, Germany, for providing the DNA of the nucleoprotein of Marburg virus. We also thank Dr. J.B. McCormick, former head of the Special Pathogens Branch, Centers Disease Control and Prevention, Atlanta, GA, for providing the inactivated authentic Marburg virus antigens for IFA. We thank Ms. M. Ogata, Department of Virology 1, National Institute of Infectious Diseases, for her technical and clerical assistance.

REFERENCES

Anonymous. 1999. Marburg fever, Democratic Republic of the Congo. Wkly Epidemiol Rec 74:145.

Bausch DG, Borchert M, Grein T, Roth C, Swanepoel R, Libande ML, Talarmin A, Bertherat E, Muyembe-Tamfum JJ, Tugume B, Colebunders R, Konde KM, Pirad P, Olinda LL, Rodier GR, Campbell P, Tomori O, Ksiazek TG, Rollin PE. 2003. Risk factors for Marburg hemorrhagic fever, Democratic Republic of the Congo. Emerg Infect Dis 9:1531–1537.

Conrad JL, Isaacson M, Smith EB, Wulff H, Crees M, Geldenhuys P, Johnston JJ. 1987. Epidemiologic investigation of Marburg virus disease, Southern Africa, 1975. Am J Trop Med Hyg 27:1210–1215.

Drosten C, Gottig S, Schilling S, Asper M, Panning M, Schmitz H, Gunther S. 2002. Rapid detection and quantification of RNA of Ebola and Marburg viruses, Lassa virus, Crimean-Congo hemorrhagic fever virus, Rift Valley fever virus, dengue virus, and yellow fever virus by real-time reverse transcription-PCR. J Clin Microbiol 40:2323–2330.

Feldmann H, Slenczka W, Klenk HD. 1996. Emerging and reemerging of filoviruses. Arch Virol Suppl 11:77–100.

Gear JS, Cassel GA, Gear AJ, Trappler B, Clausen L, Meyers AM, Kew MC, Bothwell TH, Sher R, Miller GB, Schneider J, Koornhof HJ, Gomperts ED, Isaacson M, Gear JH. 1975. Outbreake of Marburg virus disease in Johannesburg. Br Med J 4:489–493.

Ikegami T, Niikura M, Saijo M, Miranda ME, Calaor AB, Hernandez M, Acosta LP, Manalo DL, Kurane I, Yoshikawa Y, Morikawa S. 2003. Antigen capture enzyme-linked immunosorbent assay for specific detection of Reston Ebola virus nucleoprotein. Clin Diagn Lab Immunol 10:552–557.

Johnson ED, Johnson BK, Silverstein D, Tukei P, Geisbert TW, Sanchez AN, Jahrling PB. 1996. Characterization of a new Marburg virus isolated from a 1987 fatal case in Kenya. Arch Virol Suppl 11:101–114.

Ksiazek TG, Rollin PE, Williams AJ, Bressler DS, Martin ML, Swanepoel R, Burt FJ, Leman PA, Khan AS, Rowe AK, Mukunu R, Sanchez A, CJ P. 1999. Clinical virology of Ebola hemorrhagic fever (EHF): Virus, virus antigen, and IgG and IgM antibody findings among EHF patients in Kikwit, Democratic Republic of the Congo, 1995. J Infect Dis 179:S177–S187.

Martini GA, Knauff HG, Schmidt HA, Mayer G, Baltzer G. 1968. [On the hitherto unknown, in monkeys originating infectious disease: Marburg virus disease]. Dtsch Med Wochenschr 93:559–571.

Niikura M, Ikegami T, Saijo M, Kurane I, Miranda ME, Morikawa S. 2001. Detection of Ebola viral antigen by enzyme-linked immunosorbent assay using a novel monoclonal antibody to nucleoprotein. J Clin Microbiol 39:3267–3271.

Peters CJ, LeDuc JW. 1999. An introduction to Ebola: The virus and the disease. J Infect Dis 179:ix–xvi.

Saijo M, Niikura M, Morikawa S, Ksiazek TG, Meyer RF, Peters CJ, Kurane I. 2001. Enzyme-linked immunosorbent assays for detection of antibodies to Ebola and Marburg viruses using recombinant nucleoproteins. J Clin Microbiol 39:1–7.

Sanchez A, Ksiazek TG, Rollin PE, Miranda ME, Trappier SG, Khan AS, Peters CJ, Nichol ST. 1999. Detection and molecular characterization of Ebola viruses causing disease in human and nonhuman primates. J Infect Dis 179:S164–S169.

Smith DH, Johnson BK, Isaacson M, Swanapoel R, Johnson KM, Killey M, Bagshawe A, Siongok T, Keruga WK. 1982. Marburg-virus disease in Kenya. Lancet 1:816–820.